

Topological phase for entangled two-qubit states and the representation of the $SO(3)$ group

F. De Zela

Departamento de Ciencias, Sección Física
Pontificia Universidad Católica del Perú, Ap.1761, Lima, Perú.

August 12, 2018

Abstract

We discuss the representation of the $SO(3)$ group by two-qubit maximally entangled states (MES). We analyze the correspondence between $SO(3)$ and the set of two-qubit MES which are experimentally realizable. As a result, we offer a new interpretation of some recently proposed experiments based on MES. Employing the tools of quantum optics we treat in terms of two-qubit MES some classical experiments in neutron interferometry, which showed the π -phase accrued by a spin-1/2 particle precessing in a magnetic field. By so doing, we can analyze the extent to which the recently proposed experiments - and future ones of the same sort - would involve essentially new physical aspects as compared with those performed in the past. We argue that the proposed experiments do extend the possibilities for displaying the double connectedness of $SO(3)$, although for that to be the case it results necessary to map elements of $SU(2)$ onto physical operations acting on two-level systems.

PACS numbers: 03.65.Vf, 03.67.Mn, 07.60.Ly, 42.50.Dv

1 Introduction

Geometric phases and entangled states have been two of the most addressed issues during the last few years. The widespread interest on these topics embraces both theoretical and applied aspects. Since the appearance of Berry's seminal paper [1], different geometric phases have been theoretically introduced and experimentally tested. Due to some subtleties that are inherent to the above mentioned topics, the introduction of a new phase and/or its experimental demonstration eventually causes some controversy and it may take some time before an issue becomes settled. This usually requires seeing one and the same topic from different perspectives. It is in this vein that the present article deals with a topological phase recently proposed by Milman and Mosseri [2]. These authors discussed a quantum optics interference experiment designed to demonstrate a topological phase shift, which should stem from the subtleties

of the $SO(3)$ rotation group topology. Milman and Mosseri claim that by using two-qubit, maximally entangled states (MES) the double connectedness of the $SO(3)$ rotation group can be displayed. Their proposal is based on a one-to-one map between $SO(3)$ and the set of two-qubit MES. These states can be currently produced as, e.g., polarization-entangled photon pairs by using a down converter [3]. In order to measure the topological phase, one of the photons from the entangled pair is sent through a Mach-Zehnder interferometer, at whose output it is detected in coincidence with the other photon from the entangled pair, which serves as the reference mode. In one of the arms of the Mach-Zehnder interferometer a variable dephasing ϕ is introduced. The goal is to bring into evidence that there are two classes of trajectories in $SO(3)$, as followed by the MES when they are subjected to the transformations due to different devices that constitute the optical system (beam-splitters, wave plates, mirrors, etc.). As a result, the counting rate for coincidence detections at two detectors, D_1 and D_2 , put at the output ports of the interferometer, is given by $P = (1/2)|(-1)^n - \cos\phi|$. Here, n counts the number of times that the trajectory breaks on the surface of the $SO(3)$ sphere, on which such trajectories can be represented. In a sequel to Ref. [2], LiMing, Tang and Liao [4] refine the proposal of Milman and Mosseri, by showing how to realize a larger family of closed trajectories, in which the sudden jumps of the original proposal are replaced by a continuously changing path. Moreover, n can have odd and even values beyond the two only cases, $n = 0$ and $n = 1$, that Milman and Mosseri had considered. To the best of our knowledge, the proposed experiments have not yet been implemented.

One goal of the present work is to discuss the extent to which the proposal of Milman and Mosseri, or that of LiMing, Tang and Liao, would imply the appearance of a new phase. Around three decades ago a series of experiments in neutron interferometry were performed [10], whose aim was to bring into evidence the π -phase that arises when a spinor is subjected to a 2π rotation. Such a π -phase illustrates one of the most salient features characterizing the interplay between the groups $SO(3)$ and $SU(2)$. The advent of quantum optics allowed not only to extend our capability to perform new experiments on this line, but helped also to interpret the old experiments in the framework of entangled states. In this work we present an alternative interpretation of experiments similar to those proposed by Milman and Mosseri and LiMing, Tang and Liao. To this end, we re-analyze the neutron experiments by employing the tools of quantum optics, thereby recovering the known results but at the same time extending their scope. Though we refer specifically to neutron experiments, our results are valid for experiments that can be performed in quantum optics. Only minor changes are needed to obtain the corresponding predictions when one works with photons instead of dealing with fermions.

This paper is organized as follows. We first present the evolution of maximally entangled states in connection with the $SU(2)$ group. We briefly discuss those features concerning the double connectedness of $SO(3)$, which are relevant for our case. A more detailed discussion, including some technical details of $SO(3)$ has been included in the Appendix. This Appendix should serve to

make the present paper more self contained. In the next section we discuss neutron interferometry by means of a full quantum-mechanical treatment. This gives us the opportunity to stress the essential role played by entangled states in this context. We analyze in detail how the π -phase arises and compare our approach with another, newly proposed one, that makes use of the geometrical phase for mixed states. We then discuss the basic experimental arrangement - a Mach-Zehnder interferometer - necessary to bring into evidence those features of the $SO(3)$ group that have been on the focus of our interest. We summarize our results at the end of the paper and make some conclusions regarding the novelty of the recent proposals.

2 The topological phase

Two-qubit MES are given by

$$|\alpha, \beta\rangle = \frac{1}{\sqrt{2}}(\alpha |0, 0\rangle + \beta |0, 1\rangle - \beta^* |1, 0\rangle + \alpha^* |1, 1\rangle), \quad (1)$$

with $|\alpha|^2 + |\beta|^2 = 1$. Following Milman and Mosseri we define the ‘‘Hilbert space of all MES’’ as $\Omega_{MES} = \left\{ (\alpha, \beta) \in \mathbb{C}^2 / |\alpha|^2 + |\beta|^2 = 1 \text{ and } (\alpha, \beta) \sim (-\alpha, -\beta) \right\} = S^3/Z_2 = SO(3)$. First of all, let us note that what we obtain as a consequence of the identification $(\alpha, \beta) \sim (-\alpha, -\beta)$ is the well known two-to-one homomorphism between $SU(2)$ ($= S^3$) and $SO(3)$ ($= S^3/Z_2$). Our main purpose here is to elucidate whether the mathematical construction leading to Ω_{MES} has a corresponding physical realization or not. The key point is the identification $(\alpha, \beta) \sim (-\alpha, -\beta)$. It certainly reflects the physical indistinguishability between the states $|\alpha, \beta\rangle$ and $|\alpha, \beta\rangle = e^{i\pi} |\alpha, \beta\rangle$. We note that, in general, $|\alpha, \beta\rangle \neq |e^{i\psi}\alpha, e^{i\psi}\beta\rangle$, so that one could expect that the production of MES in the laboratory automatically leads to a physical realization of Ω_{MES} . However, considering the experimental production of MES, we realize that what we can produce in the laboratory are states whose global phase remains undetermined. This means that not only (α, β) and $(-\alpha, -\beta)$ are experimentally indistinguishable, but also $|\alpha, \beta\rangle$ and any other state of the form $e^{i\psi} |\alpha, \beta\rangle$. Thus, instead of Ω_{MES} , and because the set whose elements are the factors $e^{i\psi}$ is nothing but $U(1)$ ($= S^1$), what we actually produce in the laboratory seems to be rather akin to a realization of the Hopf-fibration [5] $S^3 \xrightarrow{S^1} S^2$, by which the $SU(2)$ manifold (S^3) is locally decomposed in the form of products of S^2 -elements (α, β) by elements $e^{i\psi}$ of the fiber S^1 . The precise way in which such a realization can be established is however not a matter of our concern here. For our purposes, it should suffice to point out that experimentally realizable MES are defined up to a global phase and can be put in one-to-one correspondence with the $SU(2)$ elements.

Indeed, MES given by Eq.(1) with $|\alpha|^2 + |\beta|^2 = 1$ can also be represented in

matrix form as

$$M_{(\alpha,\beta)} = \begin{pmatrix} \alpha & \beta \\ -\beta^* & \alpha^* \end{pmatrix}, \quad (2)$$

leaving aside the normalization factor $1/\sqrt{2}$. $M_{(\alpha,\beta)}$ has thus the form of a general $SU(2)$ -matrix. It is well known that any Hamiltonian of a two-level system can be written in a form that corresponds to the interaction of a spin-1/2 particle with a magnetic field: $H = -\mu \cdot \mathbf{B} \equiv \hbar\omega\sigma \cdot \mathbf{n}/2$. If such a Hamiltonian drives the evolution of one of the two qubits in Eq.(1), the result is an evolved, two-qubit state $|\alpha(t), \beta(t)\rangle$ that remains a MES. Let us first restrict ourselves to the case of a field having a constant direction \mathbf{n} . When H acts on the first qubit, the evolved state $|\alpha(t), \beta(t)\rangle$ can be obtained from the initial state $|\alpha, \beta\rangle \equiv |\alpha(0), \beta(0)\rangle$, as

$$\begin{pmatrix} \alpha(t) & \beta(t) \\ -\beta^*(t) & \alpha^*(t) \end{pmatrix} = \begin{pmatrix} A(t) & B(t) \\ -B^*(t) & A^*(t) \end{pmatrix} \begin{pmatrix} \alpha & \beta \\ -\beta^* & \alpha^* \end{pmatrix} \equiv M_U M_{(\alpha,\beta)}, \quad (3)$$

whereby the first matrix on the right-hand side corresponds to the evolution operator $U = \exp(-i\omega t(\mathbf{n} \cdot \sigma)/2) = I \cos(\omega t/2) - i\mathbf{n} \cdot \sigma \sin(\omega t/2)$ acting on the first qubit. One finds that $A(t)$ and $B(t)$ are given by just the same elements of U :

$$A(t) = \cos(\omega t/2) - in_z \sin(\omega t/2) \quad (4)$$

$$B(t) = -i(n_x - in_y) \sin(\omega t/2). \quad (5)$$

A similar expression can be obtained for the case when it is the second qubit the one which is subjected to the action of the Hamiltonian. In such a case, $|\alpha(t), \beta(t)\rangle$ is given by a relation similar to Eq.(3), but involving U^T , the transpose of U :

$$\begin{pmatrix} \alpha(t) & \beta(t) \\ -\beta^*(t) & \alpha^*(t) \end{pmatrix} = \begin{pmatrix} \alpha & \beta \\ -\beta^* & \alpha^* \end{pmatrix} \begin{pmatrix} A(t) & -B^*(t) \\ B(t) & A^*(t) \end{pmatrix} = M_{(\alpha,\beta)} (M_U)^T \quad (6)$$

As we see, the two evolutions bring an initial $SU(2)$ -element into another one, so that maximal entanglement is preserved. This is so because all the involved matrices, $M_{(\alpha,\beta)}$, M_U , and $(M_U)^T$, are elements of $SU(2)$ and by multiplying two of them what we obtain is just another element of the same group. Each matrix $M_{(\alpha,\beta)}$ can be seen as the result of applying a rotation M_U with $A = \alpha$ and $B = \beta$ to the identity matrix $M_{(\alpha=1,\beta=0)}$, which corresponds to the state $|1,0\rangle$. In other words, $M_{(\alpha,\beta)}$ can be identified with the rotation $M_{U(\alpha,\beta)}$. This way, two-qubit MES span just another representation-space for

rotations. Using it we obtain a representation which is isomorphic to the usual, one-qubit, $SU(2)$ spinor representation. For closed trajectories a π -phase might arise: e.g., when $\omega t = 2\pi$, so that $|\alpha(t), \beta(t)\rangle = -|\alpha, \beta\rangle$. This phase can only be [12], of course, a relative phase between two states (e.g., light beams), whereby one of the states is taken as a reference state. By making the two beams interfere we can bring the π -phase into evidence. This was the aim of the classical experiments in neutron interferometry which were developed in the past [10, 11]. In the following Section we shall discuss these experiments in the framework of maximally entangled states, so as to bring to the fore those features that the classical experiments have in common with the newly proposed ones. However, before going into the analysis of the neutron experiments, it seems worthwhile to briefly discuss those general matters related to the $SO(3)$ double connectedness that have prompted some recent proposals, like the ones referred to above [2, 4]. This will also set the stage for the discussion that follows. A more detailed treatment of the $SO(3)$ double connectedness and related issues has been included in the Appendix.

The double connectedness of $SO(3)$ refers to the fact that not every closed curve in the $SO(3)$ parameter space can be continuously deformed to a single point at the origin, which is the point representing the identity transformation. In other words, not every closed curve in $SO(3)$ is homotopically equivalent to a point. The curves which are homotopic to the identity belong to one homotopy class. The curves which are not homotopic to the identity belong to a second homotopy class. It happens that $SO(3)$ has only two homotopy classes. Now, if we take an object and apply to it a sequence of $SO(3)$ transformations which begin and end at the identity, we cannot tell - by just observing the object - which homotopy class the sequence belongs to. In order to identify the homotopy class we need to map the sequence of transformations into elements of $SU(2)$, the simply connected group which shares with $SO(3)$ the same Lie algebra. For each element of $SO(3)$ there are two elements of $SU(2)$ that can be mapped on it. Such a map allows us to disclose the double connectedness of $SO(3)$. These topics are discussed in more detail in the Appendix. Here, it should be enough to stress that in order to disclose the double connectedness of $SO(3)$ we do need an object on which to apply the corresponding $SU(2)$ transformations. Of course, such an object is nothing but a spin-1/2 particle or any other two-level system. We cannot remain working with $SO(3)$ transformations or with objects on which these transformations apply, if we aim at disclosing the subtleties of the $SO(3)$ topology. If that would be possible, a rigid body would suffice. Thus, the essential point concerning MES is not that they could be put in one-to-one correspondence with a set of 3-dimensional rotation matrices - which is true for rigid bodies -, but that MES entail two-level systems on which we can apply $SU(2)$ transformations. In order to disclose the subtleties of the $SO(3)$ topology we need at least three things: spinors, entanglement, and the possibility of interfering a “rotated” with a “non-rotated” spinor.

Milman and Mosseri [2] considered two sequences of transformations. Both sequences start by being applied to the identity $(\alpha, \beta) = (1, 0)$ and consist of four rotations, whereby the first two of these rotations act on the first qubit, and the

last ones on the second qubit. However, one sequence belongs to one homotopy class, bringing the point $(1, 0)$ back to itself, whereas the other sequence has $(-1, 0)$ as its endpoint and belongs to the other homotopy class. The idea is to consider sequences of rotations for which the rotation axis is not kept constant, as it was the case in the neutron experiments referred to above. According to Milman and Mosseri, by keeping the rotation axis constant the π phase detected in those experiments is not necessarily related to the “subtle nature of $SO(3)$ ”, but to “a property shared by $SO(3)$ and its subgroup $SO(2)$ ”. In order to apply those results which are valid only for a constant rotation axis, the sequence of rotations considered in [2] does not entail a continuously varying rotation axis, but it is split into four rotations. Each one of these rotations is performed about a fixed direction, which is changed from one rotation to the next. LiMing *et al.* [4] consider instead a continuously changing rotation axis $\mathbf{n}(t) = (\sin \theta \cos \omega t, \sin \theta \sin \omega t, \cos \theta)$. This particular case corresponds to a spin driven by a magnetic field which is precessing around the z -axis. The corresponding Schrödinger equation can be solved exactly in this case as well [6, 7].

Now, for our present purposes, it suffices to note that the evolution of a spinor driven by a general Hamiltonian $H(t) = \hbar\omega\sigma \cdot \mathbf{n}(t)/2$ is given by $|\psi(t)\rangle = U(t)|\psi(0)\rangle$, with $U(t) \in SU(2)$. This holds true for a general $\mathbf{n}(t)$, even though an expression for $U(t)$ is not easily obtained in closed form but in the two aforementioned cases. Hence, Eqs.(3) and (6) remain valid for a variable $\mathbf{n}(t)$, in general. These equations enable us to calculate - at least formally - the evolved MES as

$$|\alpha(t), \beta(t)\rangle = \frac{1}{\sqrt{2}} (\alpha(t)|0, 0\rangle + \beta(t)|0, 1\rangle - \beta^*(t)|1, 0\rangle + \alpha^*(t)|1, 1\rangle). \quad (7)$$

Milman and Mosseri point out one aspect of the sequences of rotations they consider. Namely, that for both sequences, irrespective of the homotopy class to which they belong, their dynamical phase vanishes. As for the Pancharatnam phase, it also vanishes, except in those cases where the evolved state “crosses the space orthogonal to the initial state, where it abruptly changes by π ” [2]. This feature is interpreted as giving further support to the contention that these π -phases have a purely topological origin.

Taking the time derivative of Eq.(7) it is easy to see that not only for the particular sequences considered by Milman and Mosseri, or for those proposed by LiMing *et al.*, but quite generally, the states $|\alpha(t), \beta(t)\rangle$ evolve in time satisfying

$$\langle \alpha(t), \beta(t) | \frac{d}{dt} |\alpha(t), \beta(t)\rangle = \frac{1}{2} \frac{d}{dt} (|\alpha(t)|^2 + |\beta(t)|^2) = 0, \quad (8)$$

which is the condition for parallel transport [9]. Furthermore,

$$\langle \alpha(0), \beta(0) | \alpha(t), \beta(t)\rangle = Re(\alpha^*(0)\alpha(t) + \beta^*(0)\beta(t)). \quad (9)$$

Hence, recalling the definition of the geometric phase,

$$\Phi_g = \arg \langle \alpha(0), \beta(0) | \alpha(\tau), \beta(\tau) \rangle + i \int_0^\tau \langle \alpha(t), \beta(t) | \frac{d}{dt} | \alpha(t), \beta(t) \rangle dt, \quad (10)$$

we see that, because the dynamical phase $-i \int_0^\tau \langle \alpha(t), \beta(t) | \frac{d}{dt} | \alpha(t), \beta(t) \rangle dt = 0$ in our case, the geometric phase Φ_g reduces to the Pancharatnam - or total - phase; i.e., $\Phi_g = \arg \langle \alpha(0), \beta(0) | \alpha(\tau), \beta(\tau) \rangle$. Whenever $|\alpha(\tau), \beta(\tau)\rangle = -|\alpha(0), \beta(0)\rangle$, the geometric phase $\Phi_g = \pi$. So we see that each time the point $(\alpha(t), \beta(t))$ is brought to the surface of the solid ball of radius π that constitutes the parameter space of $SO(3)$ (see the Appendix), it accumulates a π phase. However, we can hardly say that these increments of π in Φ_g should be interpreted as evidencing a *new* sort of phase, which would be distinctly related to the topology of $SO(3)$. All these results are indeed known since a couple of years and have been discussed within a more general framework by Sjöqvist [8], who was interested on a variable degree of entanglement. From a physical point of view, it appears to be far more interesting to study the nonclassical dependence of the geometric phase on the degree of entanglement [8], than to investigate the topology of $SO(3)$ by experimental means. Even so, and because questions related to the subtleties of the $SO(3)$ topology have recently attracted much attention, we find it necessary to analyze in detail what features the newly proposed experiments would have in common with those already performed in the past using neutrons. In the following section we employ the tools of quantum optics to analyze some representative experiments on neutron interferometry.

3 Neutron interferometry

A π -phase that arises as a consequence of a 2π rotation applied to spinors is a familiar feature of these eminently quantum-mechanical objects. The -1 factor that the corresponding wave function acquires as a consequence of such an evolution was first assumed to be unobservable, but experiments performed by Werner *et al.* [10] and by Rauch *et al.* [11] - prompted by *Gedanken* experiments discussed by Aharonov and Susskind [12] and Bernstein [13] - brought such a factor into evidence. These experiments used an unpolarized neutron beam, which was coherently split into two other beams at the entrance of an interferometer. The two beams were reflected by means of crystals, so as to bring them to a point where they recombine and interfere, before being detected. In order to make the π -phase appear, one of the two beams was subjected to the action of a tunable magnetic field, before recombining it with the other beam. Werner *et al.* [10] used two detectors, D_1 and D_2 , in order to show the sinusoidal variation of the difference in neutron counts, $N(D_1) - N(D_2)$, as a function of the magnetic field; that is, as a function of ωt , with t fixed and variable ω . The arrangement is essentially a Young's type interferometer (see Fig. (1)), in which one of the beams is subjected to a tunable dephasing.

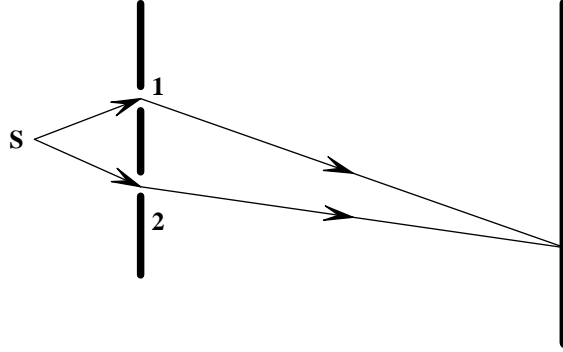


Figure 1: Two-slit Young's interferometer.

In a conventional Young's interferometer the counting rate is given by an expression of the form $N(D) \sim 1 + k \cos \varphi$, where the constant k encapsulates how the interferometer acts on the incoming beam by splitting it into two other beams, and φ is a phase arising from their path difference. The essential point that we want to stress here is the following: a full quantum-mechanical treatment of the Young's interferometer requires that we invoke a field theoretic description, with the radiation field being given by a density operator $\rho = |\psi\rangle \langle\psi|$, and the electromagnetic field being described in terms of annihilation and creation operators for each possible mode. For single-mode excitation, the Young's interference experiment can be described [14] in terms of the boson operator $b^\dagger = a_1^\dagger \cos \theta + a_2^\dagger \sin \theta$, where each a_i ($i = 1, 2$) refers to the respective pinhole of the interferometer depicted in Fig.(1). The photon state out of which the interference fringes arise is therefore given by $b^\dagger |vac\rangle = \cos \theta |1, 0\rangle + \sin \theta |0, 1\rangle$, with $|n_1, n_2\rangle$ meaning a state with n_i photons in the corresponding mode a_i . The constant k introduced above reads, for the present case [14], $k = \sin 2\theta$. For modes of equal intensity one has $\theta = \pi/4$ and the counting rate becomes $N(D) \sim 1 + \cos \varphi$, in accordance with the classical result. We see that a proper, full quantum-mechanical treatment of Young's experiment requires the appearance of the *entangled* state $b^\dagger |vac\rangle = (|1, 0\rangle + |0, 1\rangle) / \sqrt{2}$. An analogous treatment can be envisaged for neutron experiments of the sort performed by Werner *et al.* [10]. Indeed, as Silverman [15] has shown, a Mach-Zehnder charged-fermion interferometer, in which a confined magnetic field causes an Aharonov-Bohm phase-shift between the two beams, can be treated field theoretically like Young's experiment. This is also the case for the experimental arrangement of Werner *et al.*, as one can easily show. The interferometer used by Werner *et al.* (Fig. 2) can be described [16] in terms of fermion annihila-

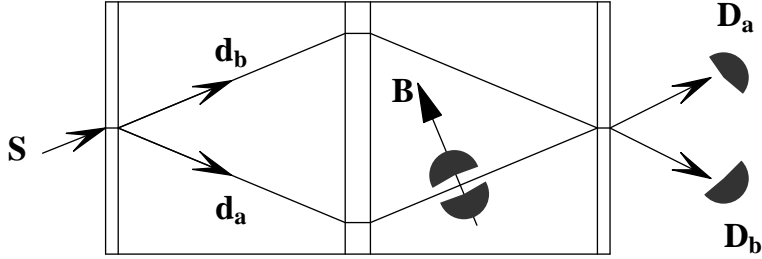


Figure 2: Neutron interferometer. There are three crystal slabs through which the neutron beams go. The first and third slab play the role of beam-splitters, whereas the second (middle) slab plays the role of the mirrors in a Mach-Zehnder interferometer. One beam passes through a tunable, transverse dc magnetic field B causing spin precession. The other beam goes through a field-free region. A 2π precession of the one beam causes a relative π -shift between the phases of the two beams.

tion operators $c_a^{out}(s)$ and $c_b^{out}(s)$, which correspond to the output states going towards detectors D_a and D_b respectively. These operators satisfy the usual anticommutation relations and can be written in terms of the input operators $d_a(s)$ and $d_b(s)$ in the usual way [16, 20]. Here, a and b refer to the two spatial modes (i.e., arms) of the interferometer and s makes explicit the dependence of the operators on the spin variables. Such an interferometer is effectively the same as a Mach-Zehnder interferometer like the one shown in Fig.(3). We can describe it in terms of the parameters characterizing the beam-splitter and the dephasing elements. We thus obtain, suppressing explicit reference to s , for brevity:

$$\begin{pmatrix} c_a^{out} \\ c_b^{out} \end{pmatrix} = \begin{pmatrix} te^{i\varphi_a} & r'e^{i\varphi_b} \\ re^{i\varphi_a} & t'e^{i\varphi_b} \end{pmatrix} \begin{pmatrix} d_a \\ d_b \end{pmatrix}, \quad (11)$$

where φ_i is the phase shift suffered by the beam going along arm $i = a, b$. The parameters r, t, r', t' , refer to the reflection and transmission amplitudes of a four-ports, lossless beam-splitter.

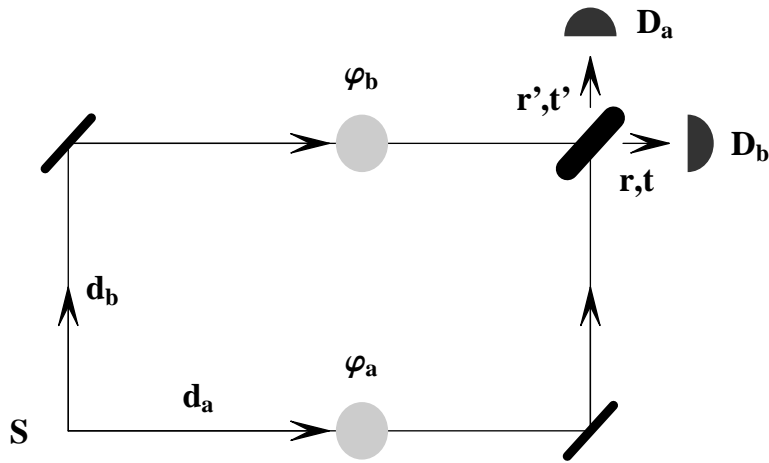


Figure 3: Mach-Zehnder interferometer in which one of the two beam-splitters has been replaced (or is represented by) a source S of entangled states. There are two dephasing elements, φ_a and φ_b . One of them can be used to make a $(-1)^n$ term appear in the coincidence counts of detectors D_a and D_b . The parameters r, t, r', t' (reflection and transmission amplitudes) characterize the four-ports, lossless beam-splitter.

The counting rates in detectors D_a and D_b are given by

$$\overline{N(D_i)} = Tr \left\{ \rho \sum_{s=\uparrow, \downarrow} (c_i^{out}(s))^\dagger c_i^{out}(s) \right\}, \quad (i = a, b), \quad (12)$$

so that, writing them in terms of d_a and d_b , we have

$$\begin{aligned} \overline{N(D_a)} &= \sum_s |t|^2 Tr(\rho d_a^\dagger(s) d_a(s)) + |r'|^2 Tr(\rho d_b^\dagger(s) d_b(s)) + 2 |t^* r' Tr(\rho d_a^\dagger(s) d_b(s))| \cos \Phi(s) \\ \overline{N(D_b)} &= \sum_s |r|^2 Tr(\rho d_a^\dagger(s) d_a(s)) + |t'|^2 Tr(\rho d_b^\dagger(s) d_b(s)) + 2 |r^* t' Tr(\rho d_a^\dagger(s) d_b(s))| \cos \Psi(s). \end{aligned}$$

Here, $\Phi(s) = \Delta\varphi(s) + \alpha + \beta$, and $\Psi(s) = \Delta\varphi(s) + \gamma + \beta$, with $\Delta\varphi(s) = \varphi_b(s) - \varphi_a(s)$, whereas the other phases are defined through the following equations: $t^* r' = |t^* r'| e^{i\alpha}$, $r^* t' = |r^* t'| e^{i\gamma}$, and $Tr(\rho d_a^\dagger d_b) = |Tr(\rho d_a^\dagger d_b)| e^{i\beta}$.

The density operator ρ that corresponds to the experimental arrangement of Werner *et al.* [10] is build up as a statistical mixture of pure, antisymmetrized states of the form $|\psi_s\rangle = (|1_s, 0\rangle - |0, 1_s\rangle)/\sqrt{2}$, with $s = \uparrow, \downarrow$ (spin up and down). It is thus given by $\rho = \sum \frac{1}{2} |\psi_s\rangle \langle \psi_s|$. On one of the two arms of the interferometer there is a magnetic field causing the spin precession that gives rise to $\Delta\varphi(s)$. Depending on whether $s = \uparrow$ or $s = \downarrow$, we have $\Delta\varphi(s) = \pm\Delta\varphi$, with $\Delta\varphi = 2\pi g_n \mu_N M \lambda B l / h^2$. We refer to [10] for the meaning of the parameters, noting only that B is the variable magnetic field and l the length over which it acts. With a ρ as given above we obtain

$$\overline{N(D_a)} = \frac{1}{2} \left(|t|^2 + |r'|^2 + |t^* r'| (\cos(\alpha - \Delta\varphi) + \cos(\alpha + \Delta\varphi)) \right) \quad (13)$$

$$\overline{N(D_b)} = \frac{1}{2} \left(|r|^2 + |t'|^2 + |r^* t'| (\cos(\gamma - \Delta\varphi) + \cos(\gamma + \Delta\varphi)) \right) \quad (14)$$

The results of Werner *et al.* can be reproduced by appropriately choosing the beam-splitter parameters, so as to mimic their experimental arrangement. Besides that, we need also to add a residual phase shift δ that is attributable to various causes, including gravity [10, 17]. Taking $|t|^2 + |r'|^2 = 2C$, $|t^* r'| = A$, $\alpha = \pi$, and $|r| = |t'| = \sqrt{A}$, $\gamma = 0$, we have

$$\overline{N(D_a)} = C - \frac{A}{2} (\cos(\delta - \Delta\varphi) + \cos(\delta + \Delta\varphi)) \quad (15)$$

$$\overline{N(D_b)} = \frac{A}{2} (1 + \cos(\delta - \Delta\varphi)) + \frac{A}{2} (1 + \cos(\delta + \Delta\varphi)), \quad (16)$$

in accordance with the results given by Werner *et al.* (see Eqs.(3) and (4) of Ref.[10]). We see therefore that the experiments in neutron interferometry,

showing the sign reversal of a spinor subjected to a 2π rotation, can be interpreted as arising from entangled states of the form $|\psi_s\rangle = (|1_s, 0\rangle - |0, 1_s\rangle)/\sqrt{2}$. In what follows, we write states of this sort as $(|\uparrow_a, 0_b\rangle - |0_a, \uparrow_b\rangle)/\sqrt{2}$, and $(|\downarrow_a, 0_b\rangle - |0_a, \downarrow_b\rangle)/\sqrt{2}$, in order to stress the analogy with the ones considered by Milman and Mosseri: $(|H_a, V_b\rangle + |V_a, H_b\rangle)/\sqrt{2}$.

Experiments like those of Werner *et al.* have been usually interpreted as putting into evidence the transformation properties of spin-1/2 particles under rotations. These rotations are represented by elements of the $SU(2)$ -manifold, the universal covering group of $SO(3)$. The one-to-one map that can be established is a map between elements of $SU(2) = S^3$ and matrices U of the form given by Eq.(2). These matrices can be taken as representing a rotation matrix, or else a MES. In fact, both cases are actually the same - as we pointed out before - because any MES can be obtained from a given, fixed one - say, $|1, 0\rangle$ - by applying to it a rotation. There is a *two-to-one* map between matrices of the form given by Eq.(2) and elements of $SO(3)$: U and $-U$ both map onto the same $R_U = R_{-U}$ in $SO(3)$.

The classical experiments in neutron interferometry have been recently analyzed in terms of *mixed state phases* by Sjöqvist *et al.* [18, 19]. These authors interpret the sign reversal of a spinor subjected to a 2π rotation as a consequence of a phase shift $\phi = \pi$, that they define in the following way:

Consider a Mach-Zehnder interferometer. To each of its arms we associate the state vectors $|a\rangle$ and $|b\rangle$, respectively. In the Hilbert space spanned by these vectors we can represent any input state, e.g., $\tilde{\rho}_{in} = |a\rangle\langle a|$, as well as the effect of mirrors, beam splitters, and relative phase shifts, by 2×2 unitary matrices \tilde{U} . The output state $\tilde{\rho}_{out}$ will then be obtained as $\tilde{\rho}_{out} = \tilde{U}\tilde{\rho}_{in}\tilde{U}^\dagger$, where \tilde{U} is the product of all those transformations suffered by the input state when it traverses the interferometer. If among these transformations there is a relative phase shift χ , the intensity I of the output beam along $|a\rangle$ can be shown [18] to be given by $\langle a|\tilde{\rho}_{out}|a\rangle$, as $I \sim 1 + \cos \chi$.

Assume now that the particles carry some internal degrees of freedom, like spin. Let $|k\rangle$, $k = 1, 2, \dots, N$, denote the vectors spanning the internal space. These vectors are assumed to be chosen so that the associated density operator ρ_0 is initially diagonal: $\rho_0 = \sum_k w_k |k\rangle\langle k|$, w_k being the classical probability to find the pure state $|k\rangle$ as part of the ensemble. The internal density operator can change inside the interferometer as described by the unitary transformation $\rho_0 \rightarrow U_i \rho_0 U_i^\dagger$. The internal state is assumed to remain unaffected by mirrors, beam splitters, etc., so that the above defined operators \tilde{U} are now extended to operators $\mathbf{U} = \tilde{U} \otimes 1_i$ that act on the full Hilbert space with basis $\{|j\rangle \otimes |k\rangle; j = a, b, k = 1, 2, \dots, N\}$. Correspondingly, an incoming state along the $|a\rangle$ -arm of the interferometer can be represented by $\rho_{in} = \tilde{\rho}_{in} \otimes \rho_0 = |a\rangle\langle a| \otimes \rho_0$. We stress that ρ_0 might correspond to a mixed state, in general. In order to define a generalization of the Pancharatnam phase to the case of mixed states Sjöqvist *et al.* [18] introduce the unitary transfor-

mation

$$\mathbf{U} = \begin{pmatrix} e^{i\chi} & 0 \\ 0 & 0 \end{pmatrix} \otimes 1_i + \begin{pmatrix} 0 & 0 \\ 0 & 1 \end{pmatrix} \otimes U_i, \quad (17)$$

which corresponds to applying the phase-shift χ along path $|a\rangle$ and U_i along path $|b\rangle$. As proved in Ref.[18], the output intensity along $|a\rangle$ is now given by

$$I \sim 1 + \nu \cos(\chi - \phi), \quad (18)$$

where the phase ϕ and the “visibility” ν are defined through

$$\text{Tr}[U_i \rho_0] = \nu e^{i\phi}. \quad (19)$$

Sjöqvist *et al.* [18] propose to take $\phi = \arg \text{Tr}[U_i \rho_0]$ as the natural generalization of the Pancharatnam phase. For a pure state $\rho_0 = |\psi_0\rangle\langle\psi_0|$ the phase ϕ reduces to the usual Pancharatnam phase between $U_i|\psi_0\rangle$ and $|\psi_0\rangle$. For a mixed state of a qubit, the corresponding density matrix can be written in terms of the Pauli matrices as $\rho = (1 + r\hat{\mathbf{r}} \cdot \boldsymbol{\sigma})/2$, with $\hat{\mathbf{r}}$ a unit vector and $r \leq 1$. The pure eigenstates $|\pm; \hat{\mathbf{r}} \cdot \boldsymbol{\sigma}\rangle$ of ρ satisfy $\rho|\pm; \hat{\mathbf{r}} \cdot \boldsymbol{\sigma}\rangle = \frac{1}{2}(1 \pm r)|\pm; \hat{\mathbf{r}} \cdot \boldsymbol{\sigma}\rangle$ and acquire Pancharatnam phases $\phi_{\pm} = \mp\Omega/2$ when $\hat{\mathbf{r}}$ traces out a geodesically closed curve on the Bloch sphere that subtends the solid angle Ω . The generalized Pancharatnam phase is given in this case by $\phi = \arg(\eta(\cos(\Omega/2) - ir \sin(\Omega/2))) = -\arctan(r \tan(\Omega/2))$; η being the common visibility of the two pure states: $\nu_+ = \nu_- \equiv \eta$. For a maximally mixed state we have $r = 0$, $\eta = |\cos(\Omega/2)|$ and $\phi = \arg(\cos(\Omega/2))$. In this case, the intensity I can be written as

$$I \sim 1 + \left| \cos\left(\frac{\Omega}{2}\right) \right| \cos\left[\chi - \arg \cos\left(\frac{\Omega}{2}\right)\right] = 1 + \cos \chi \cos\left(\frac{\Omega}{2}\right). \quad (20)$$

This formula shows that when $\Omega = 2\pi$ there is a sign change that can be traced back to the phase shift $\phi = \arg \cos \pi = \pi$. This way, the 4π symmetry of spinors, as it was tested using unpolarized neutrons, can be related to the generalized Pancharatnam phase. Eq.(20) can be compared with Eq.(16), which can be rewritten as $I \sim 1 + \cos \delta \cos \Delta\varphi$. Our δ corresponds to the relative phase-shift χ between the beams in each arm of the interferometer and which is attributable - as already said - to different causes, including gravity, while our $\Delta\varphi$ corresponds to $\Omega/2$, the phase introduced by acting on the internal degrees of freedom, i.e., on the spin, by means of a magnetic field.

At first sight, the above interpretation of the neutron experiments seems to be rather unrelated to the one given in terms of entangled states. In order to see how these two interpretations relate to one another, we resort to an alternative description [18] of the output intensity, Eq.(20), given in terms of pure state interference profiles I_k . These profiles arise as follows. Consider the pure input state $|k\rangle$. In accordance with Eq.(17), if this state goes along the $|a\rangle$ -arm of the interferometer, it suffers the change $|k\rangle \rightarrow \exp(i\chi)|k\rangle$, whereas if it goes along

the $|b\rangle$ -arm it suffers the change $|k\rangle \rightarrow U_i |k\rangle$. The output intensity associated with the input state $|k\rangle$ is then given by

$$I_k \sim |e^{i\chi} |k\rangle + U_i |k\rangle|^2 \sim 1 + |\langle k|U_i|k\rangle| \cos(\chi - \arg \langle k|U_i|k\rangle). \quad (21)$$

Now, as we have already seen in the case of Young's interferometer, the output intensity, as given by $I \sim 1 + k \cos \varphi$, can also be derived within the framework of a full quantum description. Such a description requires, however, that we resort to entangled states. The same holds true in the case of Eq.(21) and with it, also in the case of a weighted mixture of pure states, as given by $\rho_0 = \sum_k w_k |k\rangle \langle k|$. This mixed state ρ_0 gives rise to an output intensity $I = \sum_k w_k I_k$. It is then easy to see that this output intensity profile is the same as the one given by Eq.(20):

$$I = \sum_k w_k I_k \sim 1 + \sum_k w_k |\langle k|U_i|k\rangle| \cos(\chi - \arg \langle k|U_i|k\rangle) \quad (22)$$

$$= 1 + \sum_k w_k \nu_k \cos(\chi - \phi_k) = 1 + \nu \cos(\chi - \phi). \quad (23)$$

Here, $\nu_k = |\langle k|U_i|k\rangle|$, $\phi_k = \arg \langle k|U_i|k\rangle$, $\phi = \arg(\sum_k w_k \nu_k \exp(i\phi_k)) = \arg[\text{Tr}(U_i \rho_0)]$, $\nu = |\sum_k w_k \nu_k \exp(i\phi_k)| = |\text{Tr}(U_i \rho_0)|$. This way we see that the sought connection between the two interpretations occurs at the pure-state level, where a full quantum mechanical approach requires a treatment in terms of entangled states.

Next, let us calculate the number of coincident counts, $\overline{N(D_a)N(D_b)}$, for the density matrix given above. We obtain the following result:

$$\begin{aligned} \overline{N(D_a)N(D_b)} &= \text{Tr} \left\{ \rho \sum_s (c_a^{\text{out}}(s))^\dagger c_a^{\text{out}}(s) \sum_{s'} (c_b^{\text{out}}(s'))^\dagger c_b^{\text{out}}(s') \right\} \\ &= \frac{1}{2} \left\{ |rt|^2 + |r't'|^2 + 2\text{Re}[rr'(tt')^*] \right\} \\ &\quad - \frac{1}{2} \left\{ e^{i\Delta\varphi} [r^*t'|t|^2 + t^*r'|t'|^2] + e^{-i\Delta\varphi} [t'^*r|r'|^2 + tr'^*|r|^2] \right\}. \end{aligned}$$

The parameters of a lossless beam-splitter have to satisfy the equations [20] $|r|^2 + |t|^2 = 1$, and $r^*t + t'^*r' = 0$, from which it follows that $t' = t^*$ and $r' = -r^*$. Replacing these values in the above, general expression, we see that $\overline{N(D_a)N(D_b)} = 0$, as it must, because our mixed state ρ has been constructed out of one-particle states. Now, our aim is to compare a coincidence count in a neutron experiment with the one obtained with an arrangement like the one proposed by Milman and Mosseri. To this end, let us consider the case of a pure state $\rho = |\psi\rangle \langle \psi|$, with $|\psi\rangle$ given by a *two*-fermion, singlet state $|\psi\rangle = (|\uparrow_a \downarrow_b\rangle - |\downarrow_a \uparrow_b\rangle) / \sqrt{2}$.

Furthermore, let us consider an experimental arrangement like the one shown in Fig.(3), i.e., a Mach-Zehnder interferometer in which one of the two beam-splitters has been replaced by a source S of the aforementioned entangled states

$|\psi\rangle = (|\uparrow_a\downarrow_b\rangle - |\downarrow_a\uparrow_b\rangle)/\sqrt{2}$. We obtain in this case (taking $r' = r$ and $t' = t^*$, i.e., parameters corresponding to a symmetrical beam-splitter):

$$\overline{N(D_a)N(D_b)} = |t|^4 + |r|^4 + 2|rt|^2 \cos(\Delta\varphi_+ - \Delta\varphi_-), \quad (24)$$

where $\Delta\varphi_+ = \varphi_b(\uparrow) - \varphi_a(\uparrow)$, and $\Delta\varphi_- = \varphi_b(\downarrow) - \varphi_a(\downarrow)$, so that $\Delta\varphi_+ - \Delta\varphi_- = (\varphi_b(\uparrow) - \varphi_b(\downarrow)) - (\varphi_a(\uparrow) - \varphi_a(\downarrow)) \equiv \Delta\varphi_b - \Delta\varphi_a$. We have assumed that, in general, both dephasings may depend on the spin orientation. If we want to consider a case like the one corresponding to Fig.(2) it suffices to take the dephasing in arm b as being independent on the spin orientation, $\varphi_b(\uparrow) = \varphi_b(\downarrow)$, whereas $\varphi_a(\uparrow) - \varphi_a(\downarrow) = \Delta\varphi_a$. As for the beam-splitter parameters, let us take again the values corresponding to the experiments of Werner *et al.* that we chose before: $|t|^2 + |r'|^2 = 2C$, $|t^*r'| = A$, and $|r| = |t'| = \sqrt{A}$. We obtain the following expression for the number of coincident counts:

$$\overline{N(D_a)N(D_b)} = 2A^2 \{1 + \cos(\Delta\varphi_a)\}. \quad (25)$$

If we instead consider that both dephasings, φ_a and φ_b , depend on the spin orientation, we can arrange the experiment so that the dephasing in one arm, a say, becomes an integer multiple of π so as to have $\Delta\varphi_a = n\pi$. In such a case we obtain, considering again $|r| = |t'| = \sqrt{A}$,

$$\overline{N(D_a)N(D_b)} = 2A^2 \{1 + (-1)^n \cos(\Delta\varphi_b)\} \quad (26)$$

$$= 4A^2 \cos^2(\Delta\varphi_b/2), \quad \text{for } n \text{ even} \quad (27)$$

$$= 4A^2 \sin^2(\Delta\varphi_b/2), \quad \text{for } n \text{ odd.} \quad (28)$$

Thus, we see that the coincidence rate will depend on n being even or odd, as in the proposal of Milman and Mosseri. The present analysis should serve to make clear some points that in the later proposal could have caused some confusion. In the proposal of Milman and Mosseri there are three dephasing elements (properly oriented wave plates) put on three arms (modes a , b and c), respectively. The rate of coincident counts in modes a and b is predicted to be given by $P = (1/2)|(-1)^n - \cos\phi|$, where ϕ comes from a tunable dephasing element put on one arm, b , of a Mach-Zehnder interferometer. The term $(-1)^n$ comes from the dephasing introduced in the opposite arm, c , of the Mach-Zehnder interferometer and it should depend on the nature of the trajectory [2] in $SO(3)$. There is a third dephasing element, put on arm a , which lies outside the Mach-Zehnder interferometer. Now, it is the relative phase between the two arms of a Mach-Zehnder interferometer, the one upon which counting rates usually depend. One could therefore expect that a third arm is needed in order to make an extra term $(-1)^n$ appear. The arrangement depicted in Fig.(3) shows that the appearance of such a term depends instead on the possibility to drive two phases independently from one another. A third mode seems to be unnecessary, even as a reference mode, so that the arrangement shown in Fig.(3) could be used in the case of experiments with entangled photons, as well.

4 Conclusion

We have analyzed in detail different interferometric arrangements in terms of entangled states. In particular, we focussed our attention on the Mach-Zehnder interferometer as a basic tool, with the help of which some subtleties of the $SO(3)$ topology can be experimentally displayed. Experiments performed in the past with neutrons are here re-analyzed in terms of entangled states. We compared our analysis with another one which has been recently put forward, based on the geometric phase for mixed states. We showed that in both pure and mixed cases a full quantum-mechanical treatment requires the introduction of entangled states. This is so because the basic physical phenomenon behind an interferometric experiment, which is the interference pattern arising out of two states, does require the introduction of entangled states when field quantization has been invoked. This remains true for mixed states, because they are build up as a statistically weighted mixture of pure states.

We have also addressed the question as to what new features would come out by performing experiments like those proposed by Milman and Mosseri or by LiMing *et al.* A central point of their proposals is the one-to-one mapping between the elements of the set Ω_{MES} and the elements of $SO(3)$. This bijection is achieved by the identification $(\alpha, \beta) \sim (-\alpha, -\beta)$ used in the definition of the set Ω_{MES} . However, one thing is to mathematically define such a set and quite another thing is to experimentally implement it. To this end, one should be able to give a prescription as to how is it possible - at least in principle - to realize the afore said identification in a laboratory. As we stressed it before, the identification that is experimentally realized routinely is the one between (α, β) and the whole ray $e^{i\psi}(\alpha, \beta)$.

The experiments proposed by Milman and Mosseri consider subjecting one of the two beams that constitute a MES to a variable dephasing. The other beam serves as a reference one, with respect to which the phase-shift of the first beam is measured. This shift may be engineered so as to be dependent on an even or an odd multiple of π , by splitting it into two beams with the help of a Mach-Zehnder interferometer. In so far, the physics upon which the effect relies is just the same as in a classical neutron experiment: a relative π -phase difference arising out of a rotated two-level system. It is immaterial that such a two-level system be realized in practice as a spin-1/2 particle (a neutron) or as a polarized photon. Entanglement is in both cases behind the observed phenomenon. We have considered a neutron experiment designed to measure coincidence counts when one introduces independent dephasings in the two arms of a Mach-Zehnder interferometer. These coincidence counts would depend on the π -phase gained by a spinor under a 2π rotation. Such an experiment would require to feed the Mach-Zehnder interferometer with a singlet state of two fermions. To our knowledge, these experiments have not been performed. In the context of the classical neutron experiments, which were designed to reveal the π -phase, it would have been superfluous to perform such experiments with entangled, two-fermion states. Of course, their realizability with the technology that was available three decades ago is quite another question.

Present day technology offers the opportunity to develop experiments that complement those performed in the past with neutrons. The newly proposed experiments would make use of entangled states of two-level systems - polarized photons - which are not straightforwardly realized with spin-1/2 particles, like neutrons or electrons. Arrangements of the sort proposed by Milman and Mosseri - or by LiMing *et al.* - widen markedly the versatility for realizing different paths along the $SU(2)$ -manifold, when compared with the classical neutron experiments. However, to consider the predicted effects as a manifestation of a *new* topological phase seems to be, in our view, unjustified. In any case, the simple arrangement we discussed in the present work, which is illustrated in Fig.(3), should serve to make clear which essential features could be brought into evidence by experiments of this sort.

5 Appendix

Here we remind some known facts [21, 22] related to topological properties of the groups $SO(3)$ and $SU(2)$. Whereas these properties are well known, in the view of some authors [2] they could lead to misinterpretations that can be found even in textbooks. It seems thus justified to include here a very short review of some results concerning Lie groups, in order to make sure that our statements be unambiguous.

Let us first discuss in some detail the double connectedness of $SO(3)$. The Lie groups $SU(2)$ and $SO(3)$ are locally isomorphic, although globally they differ from each other. Whereas $SU(2)$ is simply connected, $SO(3)$ is not. Both groups share one and the same algebra. Among the groups sharing a given algebra, only one is simply connected. This group is called the *universal covering group*. All groups sharing a Lie algebra can be obtained from their universal covering group. To this end, one needs to determine the discrete invariant subgroups D of the simply connected group SG . The elements $d_i \in D$ satisfy $gd_i g^{-1} = d_i$ for all g in SG . After having determined D , one can construct the factor group SG/D . The factor group has the same Lie algebra as SG . When D has more than one element, SG/D is multiply connected. In our case SG is $SU(2)$, and its discrete invariant subgroup D is $Z_2 = \{I, -I\}$, where I represents the identity. Hence, $SO(3)$ is obtained from $SU(2)$ as the factor group $SU(2)/Z_2$.

It is well known that the elements of a Lie group can be obtained from the elements of its algebra by exponentiation. To any curve in the parameter space of the algebra it corresponds a curve in the parameter space of the group. Conventionally, one takes the origin of the parameter space of the group as representing the identity element. The group $SO(3)$ is a three-parameter group. It can be visualized by picturing its elements as points of a solid ball of radius π . Each point P of this ball at a distance θ from the origin represents a *counterclockwise* rotation about the axis \vec{OP} by an angle θ . Hence, antipodal points on the surface of the ball represent the same rotation. For example, in Fig.(4) points A and A' represent the same rotation. The path shown in Fig.(4) corresponds to the application of successive rotations. It starts with the

identity transformation O until it reaches the rotation represented by $A = A'$, from where it goes back to O . Although A and A' represent the same rotation, we should stress that to the jump from A to A' it corresponds a change in the rotation axis. The path shown in Fig.(5) is homotopically the same as the one shown in Fig.(4); i.e., one of these paths can be continuously deformed into the other. The path shown in Fig.(5) corresponds to a series of rotations sharing the common axis $\hat{\mathbf{z}}$.

The fact that $SO(3)$ is doubly connected can be evidenced by considering a path like the one shown in Fig.(6). It represents a series of rotations going from O to $A = A'$, from there to $B = B'$, from where one goes back to O . Such a path is homotopically the same as the paths shown in Figs.(4) and (5), when these paths have been traversed *twice*. In other words, the path shown in Fig.(5) traversed twice can be continuously deformed to the path shown in Fig.(6). This last path, in turn, can be continuously deformed to the identity. Fig.(7) shows an intermediate step of such a transformation. Any curve like \mathcal{C} is homotopically equivalent to the identity. On the contrary, a curve like the one shown in Fig.(4) is not. The double connectedness of $SO(3)$ is related to the fact that there exist paths like this last one, which cannot be deformed into a single point at O . On the other hand, the parameter space of $SU(2)$ consists of a solid ball of radius 2π , for which all points on the surface represent the same transformation: $-I$. Any closed path starting and ending at O can be continuously deformed to a single point at the origin. $SU(2)$ is thus simply connected.

The double connectedness of $SO(3)$ comes about in situations like the one illustrated in Fig.(8). It represents a series of transformations that start and end at the identity: $O \rightarrow A = A' \rightarrow O \rightarrow B' = B \rightarrow O$. For clarity, we have displaced one curve from the other, although what is meant is a series of rotations about the same axis $+\hat{\mathbf{z}}$ by the same angle π . The total angle covered along this path is therefore 4π and, as we have seen before, such a path is homotopically identical to the identity. The path shown in Fig.(9): $O \rightarrow B' = A \rightarrow O$ is homotopically identical to the identity, as well. However, in this case the first half of the path corresponds to a π -rotation about $+\hat{\mathbf{z}}$ and the second one to a π -rotation about $-\hat{\mathbf{z}}$. The two paths of Figs.(8) and (9) pertain to the same homotopy class. On the contrary, paths like the ones shown in Figs.(4) and (5) correspond to the second homotopy class. They cannot be deformed to the identity I , but are associated with the other element of Z_2 , which is $-I$.

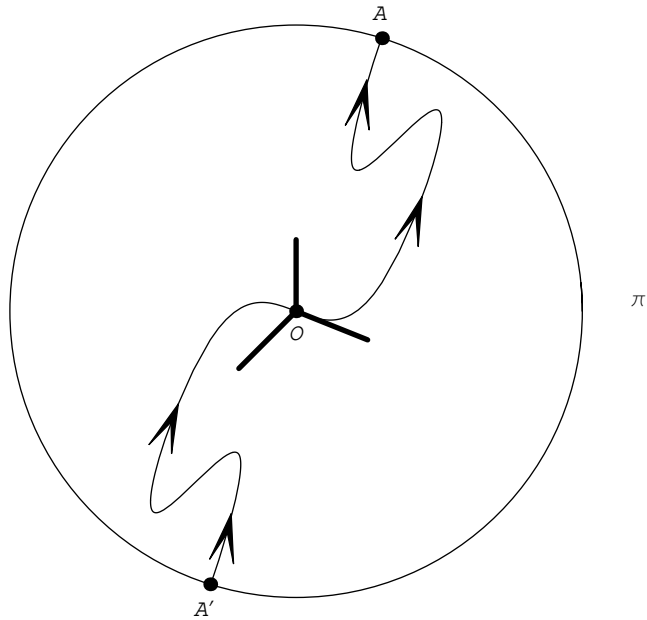
We are now ready to address the question as to how could we design an experiment that brings into evidence the double connectedness of $SO(3)$. According to what we saw, the answer reads as follows: If we want to disclose the subtleties of $SO(3)$ which are related to its double connectedness, what we need is a physical effect that clearly distinguishes the transformations I and $-I$ from one another. We need an object for which a 2π rotation would bring about a minus sign. Such an object is, of course, a spin-1/2 particle. Hence, it is precisely in order to disclose the subtleties of $SO(3)$ that we need to work with its universal covering group, which is $SU(2)$. This was the goal of the neutron

experiments [10, 11] performed three decades ago. An experiment designed to disclose the subtleties of $SO(3)$ should preferably map elements of $SU(2)$ into physical operations, not into states. In our case, the operation corresponds to an element of $SU(2)$ and it is applied to a spinor. It is essential that this spinor be part of an entangled state, in order to obtain an interference pattern from which a relative phase may be read off.

References

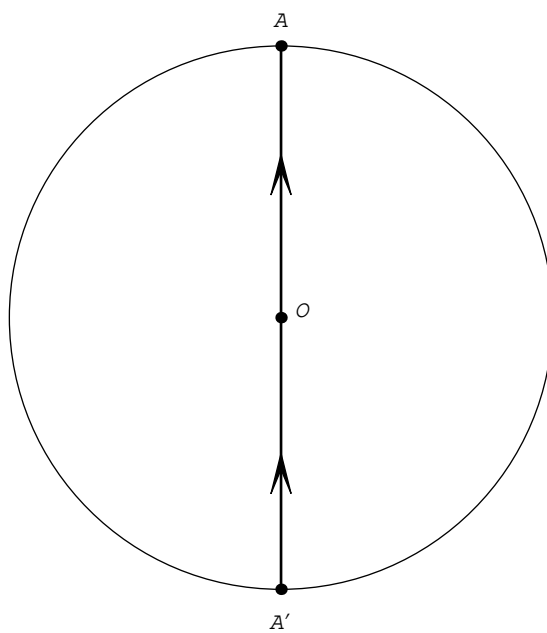
- [1] M. V. Berry, Proc. R. Soc. London, Ser. A **392**, 45 (1984).
- [2] P. Milman and R. Mosseri, Phys. Rev. Lett. **90**, 230403 (2003).
- [3] E. J. Galvez *et al.*, Am. J. Phys. **72**, 127 (2005).
- [4] W. LiMing, Z. L. Tang and C. J. Liao, Phys. Rev. A **69**, 064301-1 (2004).
- [5] R. Mosseri and R. Dandoloff, J. Phys. A **34**, 10243 (2001).
- [6] I. I. Rabi, N. F. Ramsey, and J. Schwinger, Rev. Mod. Phys. **26**, 167 (1954).
- [7] A. Bohm, A. Mostafazadeh, H. Koizumi, Q. Niu, J. Zwanziger, *The Geometric Phase in Quantum Systems*, Springer (Berlin, Heidelberg, New York 2003).
- [8] E. Sjöqvist, Phys. Rev. A **62**, 022109 (2000).
- [9] J. Anandan and L. Stodolsky, Phys. Lett. A **266**, 95 (2000).
- [10] S. A. Werner *et al.*, Phys. Rev. Lett **35**, 1053 (1975).
- [11] H. Rauch *et al.*, Phys. Lett. A **54**, 425 (1975).
- [12] Y. Aharonov and L. Susskind, Phys. Rev. **158**, 1237 (1967).
- [13] H. J. Bernstein, Phys. Rev. Lett. **18**, 1102 (1967).
- [14] D. F. Walls, Am. J. Phys. **45**, 952 (1977).
- [15] M. P. Silverman, Physica **B 151**, 291 (1988).
- [16] B. Yurke, Phys. Rev. Lett. **56**, 1515 (1986).
- [17] J.-L. Staudenmann *et al.*, Phys. Rev. A **21**, 1419 (1980).
- [18] E. Sjöqvist *et al.*, Phys. Rev. Lett. **85**, 2845 (2000).
- [19] R. Bhandari, Phys. Rev. Lett. **89**, 268901 (2002), J. Anandan *et al.*, Phys. Rev. Lett. **89**, 268902 (2002).
- [20] L. Mandel and E. Wolf, *Quantum coherence and quantum optics*, Cambridge University Press (Cambridge, New York 1995).

- [21] R. Gilmore, *Lie Groups, Lie Algebras, and Some of Their Applications*, John Wiley & Sons (New York, 1974).
- [22] D. H. Sattinger and O. L. Weaver, *Lie Groups and Algebras with Applications to Physics, Geometry, and Mechanics*, Springer (New York, 1986).



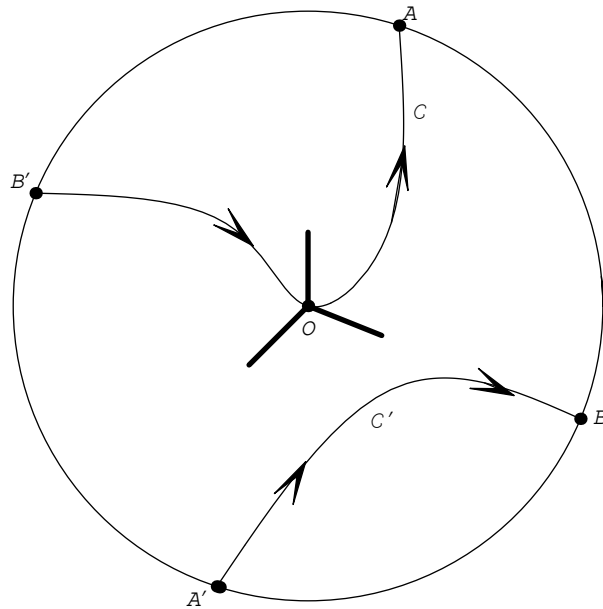
(4a)

Figure 4: The parameter space of $SO(3)$ can be represented as a solid ball of radius π . Each point P of this ball at a distance θ from the origin represents a counterclockwise rotation about axis OP by an angle θ . Antipodal points represent the same $SO(3)$ rotation. The paths shown in (a) and (b) are homotopically equivalent. They start and end at the origin (the identity) O , but cannot be continuously reduced to the identity transformation. A and A' correspond to a single group operation in $SO(3)$. In $SU(2)$, however, rotations about \hat{z} and $-\hat{z}$ can be distinguished from one another.



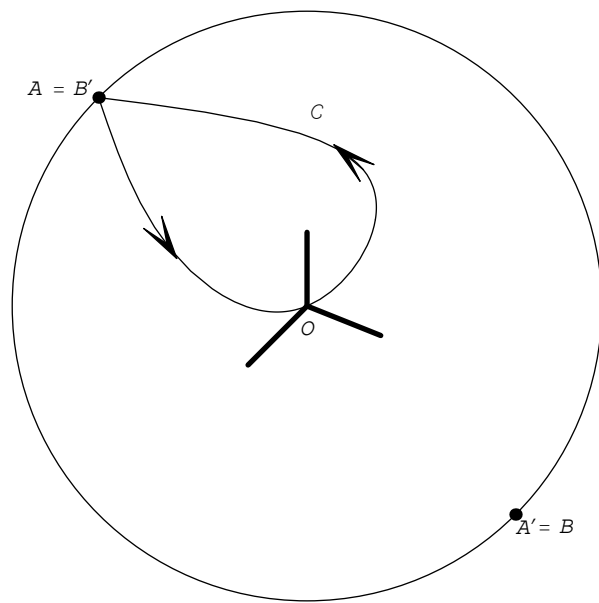
(4b)

Figure 5: Same caption as in Fig.(4).



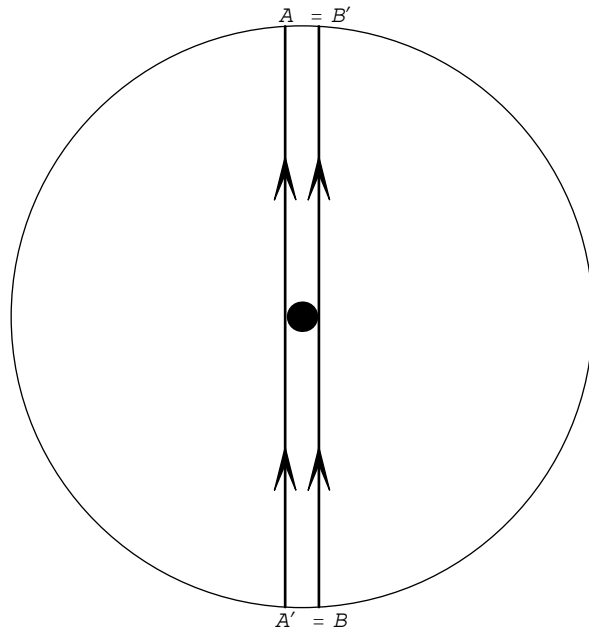
(5a)

Figure 6: The path shown in (a) starts and ends at O . It consists of a sequence of rotations that go as $O \rightarrow A = A' \rightarrow B = B' \rightarrow O$. Such a path can be continuously deformed to the identity. Part (b) of the figure shows an intermediate step towards a deformation to the identity. This path belongs to a homotopy class which is different from the one to which the path shown in Fig.(4) belongs. There are two such homotopy classes in $SO(3)$, corresponding to the double connectedness of the group.



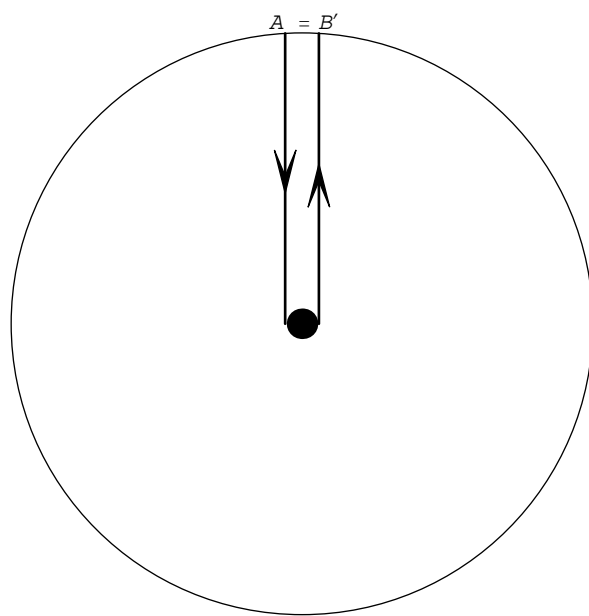
(5b)

Figure 7: Same caption as in Fig.(6).



(6a)

Figure 8: The path depicted in (a) represents a sequence of rotations about $\hat{\mathbf{z}}$. For clarity, this axis has been split into two lines. The path shown corresponds to the one of Fig.(4) when it is traversed twice. The path in this figure is then homotopically the same as the one of Fig.(6) and can be reduced to the identity. The path shown in (b) can be deformed to the identity, as well. However, (a) corresponds to a sequence of rotations about $\hat{\mathbf{z}}$, whereas in (b) half of the path corresponds to rotations about $-\hat{\mathbf{z}}$.



(6b)

Figure 9: Same caption as in Fig.(8).